

Cosmic variance of the 21-cm global signal

Julian B. Muñoz^{1,*} and Francis-Yan Cyr-Racine^{2,†}

¹*Department of Physics, Harvard University, 17 Oxford Street, Cambridge, Massachusetts 02138, USA*

²*Department of Physics and Astronomy, University of New Mexico, 210 Yale Blvd NE, Albuquerque, New Mexico 87106, USA*



(Received 21 May 2020; accepted 22 December 2020; published 6 January 2021)

Cosmological measurements of the 21-cm line of neutral hydrogen are poised to dramatically enhance our understanding of the early universe. In particular, both the epochs of reionization and cosmic dawn remain largely uncharted, and the 21-cm signal is one of the few probes to reach them. Conceptually, the simplest 21-cm measurement is the global signal (GS), which corresponds to the averaged absorption or emission of 21-cm photons across the entire sky. While bright radio foregrounds swamp the cosmic signal over the entire frequency range observable, presenting a formidable hurdle, they can in principle be subtracted, given enough sensitivity. Here, however, we point out an additional—and irreducible—source of uncertainty for the 21-cm GS: cosmic variance. The cosmic-variance noise arises from the finite volume of the universe accessible to 21-cm experiments. Due to the cosmological redshifting of 21-cm photons, each observed frequency probes our universe during a particular cosmic age, corresponding to a narrow redshift slice. The presence of large 21-cm fluctuations makes the GS within each slice different than the GS averaged over the entire universe. We estimate the size of this cosmic-variance noise, and find that for a standard scenario it has a size of ~ 0.1 mK, which is $\sim 10\%$ of the size of the expected instrumental noise of a year-long experiment. Interestingly, cosmic variance can overtake instrumental noise for scenarios with extreme 21-cm fluctuations, such as those suggested to explain the sharpness of the claimed EDGES detection. Moreover, as large-scale 21-cm fluctuations are coherent over long distances, cosmic variance correlates the measurements of the GS at nearby redshifts, leading to off-diagonal uncertainties that have so far been neglected.

DOI: [10.1103/PhysRevD.103.023512](https://doi.org/10.1103/PhysRevD.103.023512)

The first stars formed a few hundred million years after the big bang, during the epoch we call cosmic dawn. Their birth sourced abundant Lyman- α radiation, which allowed hydrogen to absorb 21-cm photons from the cosmic-microwave background (CMB). Subsequently, x-rays heated up the intergalactic hydrogen, which prompted it to emit 21-cm photons, while ultraviolet photons progressively ionized it until no hyperfine transitions were possible. Tracing the evolution of this 21-cm signal across cosmic dawn, which roughly covers the redshift range $z \approx 12$ – 25 (100–400 million years after the big bang), and the successive epoch of reionization (EoR), at $z \approx 6$ – 12 (up to a billion years after the big bang), is imperative to understand of the astrophysics of the early universe [1–8].

A promising 21-cm measurement is so-called global signal (GS), which traces the average absorption or emission of 21-cm photons across the entire cosmos [9–14]. A broad landscape of experiments are targeting this signal, such as EDGES [15], LEDA [16], SARAS [17], PRIZM [18], and SCHI-HI [19]. Their main obstacles are

radio foregrounds (mainly Galactic synchrotron emission), which shine brighter than the cosmic 21-cm signal in the radio band [20–23]. Thus, any analysis ought to simultaneously subtract these large foregrounds from the data when searching for the cosmological signal. Moreover, the presence of bright foregrounds, even if adequately subtracted, leaves thermal (Gaussian) noise in the cleaned data [24,25]. This noise can be reduced by increasing the observation time, which allows for a cosmological detection of the 21-cm GS.

In this paper we will show that, in addition to thermal noise, the 21-cm GS suffers from cosmic variance, which produces an irreducible—and previously neglected—source of noise. A 21-cm GS experiment does not have access to the entire volume of the universe at each observed frequency ν , as the universe evolves over time. At a particular ν (or z) only a small slice of the universe is integrated to obtain the 21-cm GS. The particular value measured is, thus, drawn from a random distribution around the true GS, albeit with a nonzero variance due to the 21-cm fluctuations. This is illustrated in Fig. 1, where we show the output of a 21-cm simulation averaged over two of the three physical dimensions, which reproduces the procedure of

*juliannmunoz@fas.harvard.edu
†fycr@unm.edu

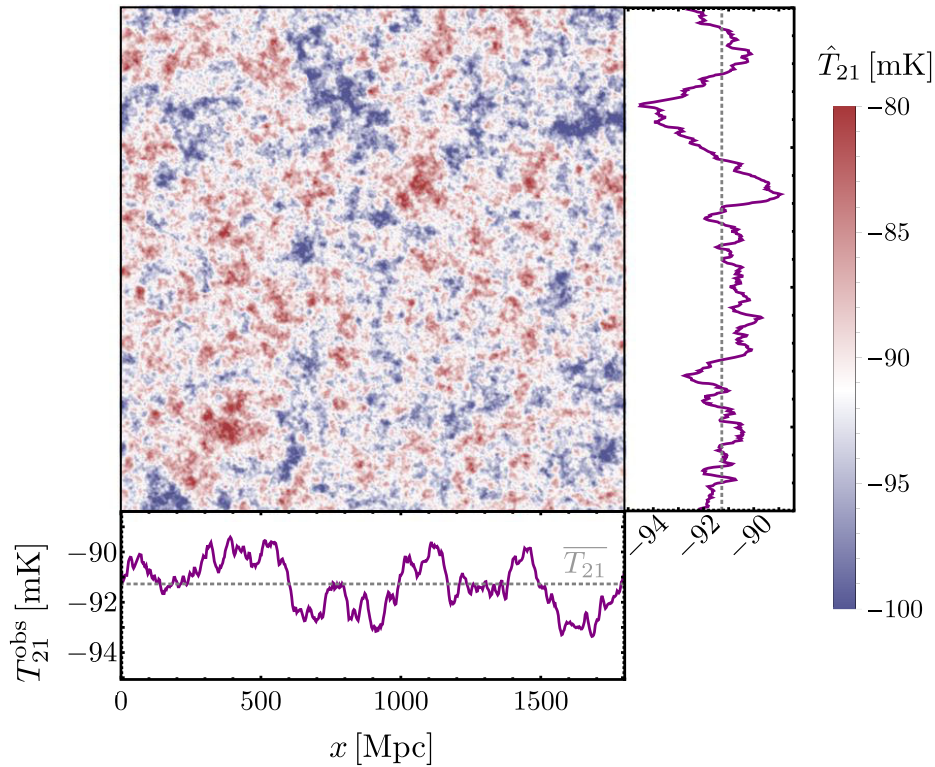


FIG. 1. The heat map shows the 21-cm temperature averaged over one of the directions of our simulation, \hat{T}_{21} , at redshift $z = 16.8$. This map is further averaged over one more of the directions to obtain the purple lines in the side panels, which correspond to the 21-cm global signal (GS) that would be observed by an experiment with a 0.1 MHz bandwidth (which yields slices 3 comoving Mpc in width). The gray dotted line shows the “true” GS, \overline{T}_{21} , obtained by averaging over the entire box. This figure illustrates how the GS measured over a thin slice can significantly depart from the true GS, giving rise to cosmic variance. Moreover, the GS is correlated if measured at nearby slices, corresponding to close-by redshifts, for distances as high as ≈ 100 Mpc (or $\Delta\nu \approx 4$ MHz at $\nu = 80$ MHz).

measuring the GS. We only have access to one of such measurements, which need not coincide with the true GS, as they fluctuate around it, at the percent-level for this simulation. This is akin to other cosmological observables (such as galaxy or cluster counts [26–30], where this effect is often termed sample variance, as well as their correlation functions [31], weak-lensing maps [32], and more famously the CMB [33,34]), where the finite cosmic volume observed presents a noise floor, which however had not been computed before for the 21-cm GS (although it had for the 21-cm power spectrum [35,36]). Moreover, as clear from Fig. 1, the 21-cm GS that would be measured at adjacent distances is correlated, as the same long-wavelength modes affect them, giving rise to cosmic covariance between measurements of the 21-cm GS at nearby redshifts.

We begin defining the relevant quantities that we will use throughout this work. Our observable is the 21-cm brightness temperature T_{21} , given by the amount of photons that neutral hydrogen absorbs from the CMB, if $T_{21} < 0$, or emits, if $T_{21} > 0$. Throughout this text we will obtain this quantity from 21cmvFAST quasineumerical simulations [37,38], based on 21cmFAST [39–42]. We share the output of our simulations as Supplementary Material [43].

The 21-cm GS $\overline{T}_{21}(z)$ is defined as the average 21-cm temperature across the universe at each redshift z . Therefore, the 21-cm temperature at any point \mathbf{x} can be generically decomposed as

$$T_{21}(\mathbf{x}, z) = \overline{T}_{21}(z) + \delta T_{21}(\mathbf{x}, z), \quad (1)$$

where $\delta T_{21}(\mathbf{x}, z)$ is the 21-cm fluctuation. In practice, however, we do not have access to the entire universe at each z . Points further from us are observed at earlier cosmic times, and thus at higher z . Measuring the GS at a particular z then implies integrating over a thin shell of the universe at a comoving distance $\chi(z)$ away from us. Mathematically, the observed 21-cm GS is given by

$$T_{21}^{\text{obs}}(z) = \int d^3\mathbf{x} W_z(\mathbf{x}) T_{21}(\mathbf{x}, z), \quad (2)$$

where $W_z(\mathbf{x})$ is the window function, which accounts for the geometry of the finite observation region. A simple example, and the one on which we will focus, is that of a 21-cm experiment observing the full sky, with a top-hat selection function in the radial direction with width

$\Delta\chi \ll \chi(z)$, although our formalism holds for any selection function.

Integrating over only part of the universe at each z means that the 21-cm fluctuation δT_{21} need not average out, which contaminates our GS measurement. We illustrate this point in Fig. 1, where we show the 21-cm signal from one of our simulations averaged over thin slices across either the x or y directions. Each of these slices provides an estimator for the 21-cm GS, T_{21}^{obs} , which clearly varies from one slice to another, illustrating how having access to a finite cosmological volume, and a single realization of the universe, produces an intrinsic variance to the GS. This is an example of cosmic variance.

We find the size of the cosmic variance by studying how much T_{21}^{obs} fluctuates around the true GS. First, it is clear from Eqs. (1), (2) that the ensemble average (denoted by brackets) of the observed global signal is unbiased, $\langle T_{21}^{\text{obs}} \rangle = \overline{T_{21}}$, by construction. There will be, however, a nonzero variance for our estimator T_{21}^{obs} . This variance is given by the autocorrelation (i.e., the zero-lag two-point function) of the observed 21-cm GS,

$$\sigma_{21}^2(z) = \langle [T_{21}^{\text{obs}}(z)]^2 \rangle - \langle T_{21}^{\text{obs}}(z) \rangle^2, \quad (3)$$

which can be computed in Fourier space as

$$\sigma_{21}^2(z) = \int \frac{d^3k}{(2\pi)^3} P_{21}(k, z) \mathcal{W}_z^2(\mathbf{k}), \quad (4)$$

in terms of the power spectrum P_{21} of the 21-cm fluctuations. Here, $\mathcal{W}_z(\mathbf{k})$ is the Fourier transform of $W_z(\mathbf{x})$, which for our simple radial top-hat is given by $\mathcal{W}_z(k) \approx j_0[k\chi(z)]$. This result is isotropic in k , as we are integrating over the entire sphere, although the same is true for half of the sphere, which is closer to the actual selection function of a global-signal experiment.

Equation (4) is the key result of this work, and it encapsulates the main insight: the 21-cm fluctuations produce an irreducible source of theoretical noise on the global signal. In order to evaluate this cosmic-variance noise we ought to know the 21-cm power spectrum P_{21} , which we obtain through 21cmvFAST simulations. In particular, large-scale fluctuations (with small k) are most important, as small-scale (large- k) modes are averaged within the observed region, so the window function in Eq. (4) suppresses their contribution to the integral. Large-scale modes are difficult to measure in simulations, due to finite-volume effects. In order to model them, we will approximate the 21-cm fluctuations as tracing the matter overdensities δ_m at large scales

$$\delta T_{21}(\mathbf{x}, z) = b_m(z) \delta_m(\mathbf{x}, z), \quad (5)$$

with a bias coefficient $b_m(z)$ that we fit to our simulation results. As our simulations have low noise for large k , we

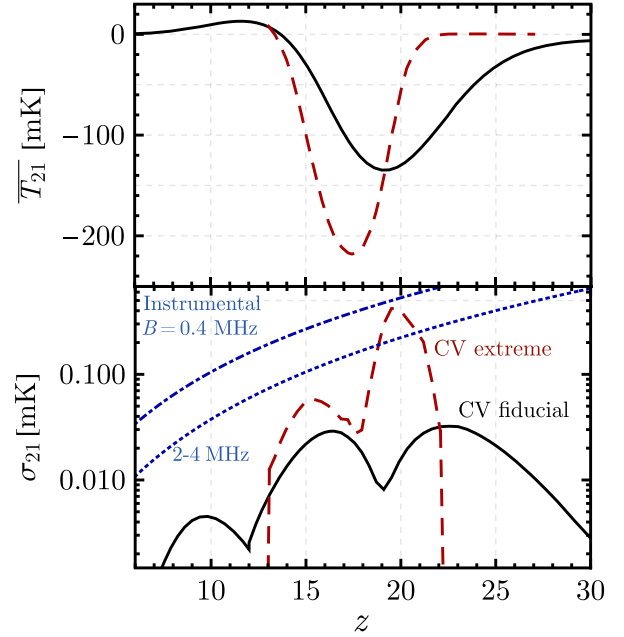


FIG. 2. Top: global signal as a function of redshift z for our fiducial model (in black) and that of Ref. [44] (in red dashed), which was designed to grow extremely fast to fit the sharpness of the EDGES detection. Bottom: noise on the 21-cm GS at each individual z . The black and red-dashed lines represent the cosmic-variance (CV) noise that we calculate for our fiducial model and for the extreme model of Ref. [44], respectively. For comparison, we also show the instrumental noise for a GS experiment observing for $t_{\text{obs}} = 1$ yr as blue lines. The upper (dash-dotted) line assumes a bandwidth $B = 0.4$ MHz, whereas the lower (dotted) line has a variable $B = 2-4$ MHz chosen to produce a comoving width $\Delta\chi = 60$ Mpc, where the cosmic covariance between bins is halved.

divide our data—and thus all integrals—into two regimes: for $k \geq 0.02$ Mpc $^{-1}$ we will directly interpolate from our simulations, whereas for $k < 0.02$ Mpc $^{-1}$ we will fit for b_m to overcome the simulation noise, although we have checked that interpolating at all k only changes the result by 10%. We show an alternate parametrization in the Supplementary Material [43], where the 21-cm fluctuations trace the relative velocities, which yields consistent results.

We show the resulting cosmic variance in Fig. 2, along with the global signal for our fiducial parameters. The size of the cosmic variance tracks the amplitude of 21-cm fluctuations, which grows at the beginning of cosmic dawn ($z \approx 25$), due to the sourcing of Lyman- α photons, and nearly vanishes during the transition from the Lyman- α coupling to X-ray heating ($z \approx 20$), where the 21-cm global signal reaches a minimum. Likewise, the fluctuations grow during the epoch of X-ray heating, and turn around as the entire cosmos is heated (by $z \approx 12$). Finally, the EoR sees another growth of fluctuations, as the hydrogen becomes inhomogeneously ionized, and eventually both the 21-cm GS and the fluctuations disappear by $z \approx 6$.

The cosmic variance for our fiducial model reaches values of $\sigma_{21} \approx 0.05$ mK. This is to be compared with the instrumental noise for an experiment targeting the 21-cm GS. We find this noise with the standard radiometer equation [11],

$$\sigma_{\text{inst}}(z) = \frac{T_{\text{sky}}(z)}{\sqrt{Bt_{\text{obs}}}}, \quad (6)$$

where B is the experimental bandwidth, t_{obs} the total observation time, and T_{sky} the sky temperature, dominated by foregrounds. We take this last quantity to be $T_{\text{sky}} = a_0(\nu/\nu_0)^{-2.5}$, with $a_0 = 1570$ K at $\nu_0 = 72$ MHz, in order to match the EDGES data [15]. We show, in Fig. 2, the instrumental noise for a standard GS experiment with $t_{\text{obs}} = 1$ year, and $B = 0.4$ MHz, as that is the resolution of the public EDGES data. Additionally, we show the noise for broader bins, designed to span a comoving distance of 60 Mpc, as we will show later that is the typical correlation length of the GS cosmic variance. Those bins have variable widths as a function of redshift, ranging from $B = 4$ MHz at $z = 6$ to 2 MHz at $z = 27$, and produce a noise comparable in size to the cosmic variance for our fiducial case (and we note that the cosmic-variance noise is roughly independent of the bandwidth as long as $\Delta\chi \ll \chi$). As clear from Eq. (4), the size of the CV noise grows with the amplitude of the 21-cm power spectrum, which is as of yet unmeasured, so models with more marked fluctuations will exhibit larger cosmic variance. As an example, we calculate the cosmic variance that would arise in the model of Ref. [44], where the parameters of the first galaxies are modified to match the timing of the claimed EDGES detection [15] (albeit not its depth). We show their global signal in Fig. 2 along ours, which evolves very rapidly during cosmic dawn. This produces dramatic 21-cm fluctuations, two orders of magnitude larger than in our fiducial model [44]. As a consequence, the expected cosmic-variance noise, which we compute and show in Fig. 2, grows and can become comparable to the instrumental noise, showcasing the importance of including cosmic variance in the analysis of the 21-cm GS. We note that, as before, we have fitted the low- k part of the power spectrum to follow matter fluctuations, although for this model we do not have all the low- k data to establish if this was a good fit. In addition, this model only fits the timing of the EDGES signal, and the power spectrum would be a factor of 6 larger if the EDGES anomalous depth was confirmed [44].

So far we have focused on the cosmic variance of the 21-cm GS at individual redshifts, as shown for instance in Fig. 2. Nevertheless, cosmic variance will also induce correlations between measurements of the 21-cm GS at nearby redshifts, as those are coherently affected by the same long-wavelength fluctuations. As opposed to instrumental noise, this will give rise to a nondiagonal covariance

matrix (see Refs. [25,45] for nondiagonal matrices due to foregrounds and beam effects). To compute it, we start with Eq. (3), although evaluated at two different redshifts z_1 and z_2 ,

$$\sigma_{21}^2(z_1, z_2) = \langle T_{21}^{\text{obs}}(z_1)T_{21}^{\text{obs}}(z_2) \rangle - \overline{T_{21}}(z_1)\overline{T_{21}}(z_2) \quad (7)$$

Now the two $T_{21}^{\text{obs}}(z_i)$ signals (and as a consequence the window functions W_{z_i} inside the brackets) can have different supports. Again going to Fourier space we obtain a generalization of Eq. (4),

$$\sigma_{21}^2(z_1, z_2) = \int \frac{d^3k}{(2\pi)^3} P_{21}(k, z_1, z_2) \mathcal{W}_{z_1}(k) \mathcal{W}_{z_2}(k), \quad (8)$$

where $P_{21}(k, z_1, z_2)$ is the power spectrum of 21-cm fluctuations at z_1 and z_2 . While this quantity can, in principle, be computed from simulations, the procedure is computationally costly. Instead, we will use Eq. (5) for $k < 0.02$ Mpc $^{-1}$, and simply assume that $P_{21}(k, z_1, z_2) = \sqrt{P_{21}(k, z_1)P_{21}(k, z_2)}$ for $k \geq 0.02$ Mpc $^{-1}$. This last approximation does not affect our results significantly, as the integral is dominated by lower k . In order to build intuition, let us study the case of two adjacent slices of our cosmos, centered at χ and $\chi + \delta\chi$ (or z and $z + \delta z$ in redshift). There we can approximate

$$\mathcal{W}_{z+\delta z}(k) = j_0[k\chi + \delta\chi] \approx \mathcal{W}_z(k) \cos(k\delta\chi), \quad (9)$$

for $\delta\chi \ll \chi$. Under that approximation it is clear that the cosmic covariance between redshifts will be suppressed for large separations δz , although, as expected, 21-cm fluctuations with small k will correlate slices that are roughly as far as $\delta\chi \sim k^{-1}$.

We show, in Fig. 3, the (normalized) correlation between measurements of the 21-cm GS at 80 MHz ($z = 16.8$), within the band of most GS experiments, and other frequencies. Nearby measurements are positively correlated, whereas for displacements $\Delta\nu \approx 10$ MHz (or $\Delta\chi \approx 200$ Mpc) the correlation becomes slightly negative, and vanishes at infinity. Displacements of $\chi_{\text{corr}} \approx 60$ Mpc are sufficient to halve the correlation, roughly independently of the central redshift.

The cosmic variance that we have calculated acts as an additional noise term in the GS covariance matrix, which has several effects. First, cosmic-variance noise will decrease the significance of any detection, by increasing the error budget. We find that for our fiducial 21-cm model, and a year-long campaign to detect the GS this is only a percent-level effect, although for an extreme model (as the one from Ref. [44] presented above) it produces a degradation of 70%. Further, we find that for our model the cosmic-variance limit, with no instrumental noise, boasts a signal-to-noise ratio $\approx 10^4$, roughly given by $\overline{T_{21}}/\sigma_{21}$, which albeit very large is finite. Second, the inferred

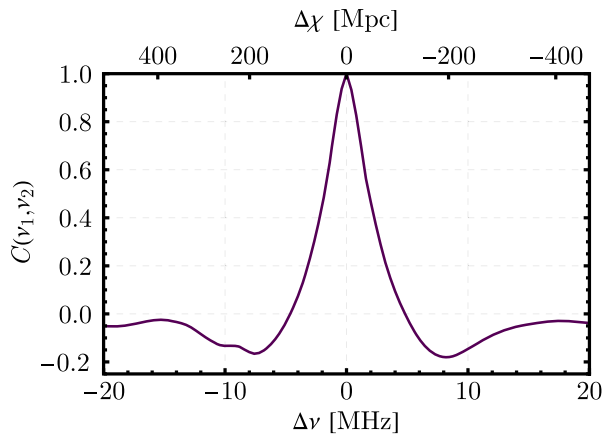


FIG. 3. Normalized correlation, $C(\nu_1, \nu_2) = \sigma_{21}^2(\nu_1, \nu_2) / [\sigma_{21}(\nu_1)\sigma_{21}(\nu_2)]$, between the 21-cm GS measured at $\nu_1 = 80$ MHz ($z_1 = 16.8$) and other frequencies $\nu_2 = \nu_1 + \Delta\nu$, separated by multiples of 0.4 MHz. In the top x axis we mark the comoving distance between frequencies, where positive numbers move upwards in redshift. Slices up to $\Delta\nu \sim 10$ MHz (or $\Delta\chi \sim 200$ Mpc) are correlated with each other, although the correlation drops by half by $\chi_{\text{corr}} = 60$ Mpc.

parameters of the 21-cm model will have underestimated errors. This underestimation again ranges from 1% for our case with mild fluctuations to nearly 100% for the extreme case. Furthermore, confirming the presence of cosmic variance would open the door to an indirect measurement of the 21-cm fluctuations integrated over low- k .

As hinted above, a determinant factor for the size of the large-scale 21-cm fluctuations—and thus the cosmic-variance noise—is how quickly the global signal evolves. This allows for a heuristic calculation of the cosmic variance with the simple shape $\sigma_{21, \text{approx}}(z) = a \times d\bar{T}_{21}/dz$, with an

amplitude $a \simeq 10^{-3}$ roughly independent of the particular GS model assumed.

While we have focused on the cosmic variance of the 21-cm GS in isolation, the same effect will create a cross-correlation between the 21-cm GS and the power spectrum. Thus, joint analyses of these two observables, as proposed in, e.g., Ref. [14], ought to include cosmic covariance.

As a byproduct of this work we have performed the largest cosmic-dawn and EoR simulations to date (although not the highest-resolution ones, e.g., [46–49]), with a box size of $L = 1.8$ Gpc comoving in 21cmvFAST. Such large box sizes were required to find the long-wavelength behavior of the 21-cm fluctuations, which determines the size of the cosmic variance, as well as the correlation between bins. This has provided clarity about the small- k behavior of the 21-cm power spectrum. We emphasize, nonetheless, that the cosmic-variance effect presented here does not rely on the details of the algorithm in 21cmvFAST/21cmFAST, and could be computed with any other simulated or analytic power spectrum. Moreover, while we have computed the cosmic variance using analytic methods, we show in the Supplementary Material [43] that our formalism agrees with the direct variance observed in simulations.

In summary, the 21-cm GS suffers from cosmic variance, similar to other cosmological observables. In this paper we have presented this effect in detail for the first time, and computed its size. While it is unlikely to hamper a first detection of the 21-cm GS, cosmic variance provides an irreducible source of noise that has to be taken into account. Doing so brings us one step closer to understanding cosmic dawn and the epoch of reionization at the percent level.

We are thankful to Alexander Kaurov, Adrian Liu, and Andrei Mesinger for discussions. J. B. M. is funded by NSF Grant No. AST-1813694.

-
- [1] P. Madau, A. Meiksin, and M. J. Rees, 21-CM tomography of the intergalactic medium at high redshift, *Astrophys. J.* **475**, 429 (1997).
 - [2] R. Barkana and A. Loeb, In the beginning: The first sources of light and the reionization of the Universe, *Phys. Rep.* **349**, 125 (2001).
 - [3] N. Yoshida, T. Abel, L. Hernquist, and N. Sugiyama, Simulations of early structure formation: Primordial gas clouds, *Astrophys. J.* **592**, 645 (2003).
 - [4] S. Furlanetto, S. P. Oh, and F. Briggs, Cosmology at low frequencies: The 21 cm transition and the high-redshift universe, *Phys. Rep.* **433**, 181 (2006).
 - [5] J. R. Pritchard and A. Loeb, Evolution of the 21 cm signal throughout cosmic history, *Phys. Rev. D* **78**, 103511 (2008).
 - [6] J. R. Pritchard and A. Loeb, 21-cm cosmology, *Rep. Prog. Phys.* **75**, 086901 (2012).
 - [7] A. Loeb and S. R. Furlanetto, *The First Galaxies in the Universe* (Princeton University Press, Princeton, NJ, 2013).
 - [8] V. Bromm and N. Yoshida, The first galaxies, *Annu. Rev. Astron. Astrophys.* **49**, 373 (2011).
 - [9] P. Shaver, R. Windhorst, P. Madau, and A. de Bruyn, Can the reionization epoch be detected as a global signature in the cosmic background?, *Astron. Astrophys.* **345**, 380 (1999), <http://articles.adsabs.harvard.edu/pdf/1999A%26A...345..380S>.
 - [10] S. Furlanetto, The global 21 centimeter background from high redshifts, *Mon. Not. R. Astron. Soc.* **371**, 867 (2006).
 - [11] J. R. Pritchard and A. Loeb, Constraining the unexplored period between the dark ages and reionization with observations of the global 21 cm signal, *Phys. Rev. D* **82**, 023006 (2010).

- [12] J. Mirocha, G. J. A. Harker, and J. O. Burns, Interpreting the global 21-cm Signal from high redshifts. II. Parameter estimation for models of galaxy formation, *Astrophys. J.* **813**, 11 (2015).
- [13] A. Cohen, A. Fialkov, R. Barkana, and M. Lotem, Charting the parameter space of the global 21-cm signal, *Mon. Not. R. Astron. Soc.* **472**, 1915 (2017).
- [14] A. Liu and A. R. Parsons, Constraining cosmology and ionization history with combined 21 cm power spectrum and global signal measurements, *Mon. Not. R. Astron. Soc.* **457**, 1864 (2016).
- [15] J. D. Bowman, A. E. E. Rogers, R. A. Monsalve, T. J. Mozdzen, and N. Mahesh, An absorption profile centred at 78 megahertz in the sky-averaged spectrum, *Nature (London)* **555**, 67 (2018).
- [16] D. C. Price *et al.*, Design and characterization of the large-aperture experiment to detect the dark age (LEDA) radiometer systems, *Mon. Not. R. Astron. Soc.* **478**, 4193 (2018).
- [17] S. Singh, R. Subrahmanyam, N. U. Shankar, M. S. Rao, B. S. Girish, A. Raghunathan, R. Somashekar, and K. S. Srivani, SARAS 2: A spectral radiometer for probing cosmic dawn and the epoch of reionization through detection of the global 21 cm signal, *Exper. Astron.* **45**, 269 (2018).
- [18] L. Philip, Z. Abdurashidova, H. C. Chiang, N. Ghazi, A. Gumba, H. M. Heilgendorff, J. M. Jáuregui-García, K. Malepe, C. D. Nunhokee, J. Peterson, J. L. Sievers, V. Simes, and R. Spann, Probing radio intensity at high-Z from marion: 2017 instrument, *J. Astron. Instrum.* **8**, 1950004 (2019).
- [19] T. C. Voytek, A. Natarajan, J. M. Jáuregui García, J. B. Peterson, and O. López-Cruz, Probing the dark ages at $z \sim 20$: The SCI-HI 21 cm all-sky spectrum experiment, *Astrophys. J.* **782**, L9 (2014).
- [20] A. E. Rogers and J. D. Bowman, Spectral index of the diffuse radio background measured from 100 to 200 MHz, *Astron. J.* **136**, 641 (2008).
- [21] G. Bernardi *et al.*, Foregrounds for observations of the cosmological 21 cm line: I. First Westerbork measurements of Galactic emission at 150 MHz in a low latitude field, *Astron. Astrophys.* **500**, 965 (2009).
- [22] A. de Oliveira-Costa, M. Tegmark, B. Gaensler, J. Jonas, T. Landecker, and P. Reich, A model of diffuse galactic radio emission from 10 MHz to 100 GHz, *Mon. Not. R. Astron. Soc.* **388**, 247 (2008).
- [23] G. Bernardi, J. Zwart, D. Price, L. Greenhill, A. Mesinger, J. Dowell, T. Eftekhari, S. Ellingson, J. Kocz, and F. Schinzel, Bayesian constraints on the global 21-cm signal from the Cosmic Dawn, *Mon. Not. R. Astron. Soc.* **461**, 2847 (2016).
- [24] G. J. Harker, J. R. Pritchard, J. O. Burns, and J. D. Bowman, An MCMC approach to extracting the global 21-cm signal during the cosmic dawn from sky-averaged radio observations, *Mon. Not. R. Astron. Soc.* **419**, 1070 (2012).
- [25] A. Liu, J. R. Pritchard, M. Tegmark, and A. Loeb, Global 21 cm signal experiments: A designer's guide, *Phys. Rev. D* **87**, 043002 (2013).
- [26] W. Hu and A. V. Kravtsov, Sample variance considerations for cluster surveys, *Astrophys. J.* **584**, 702 (2003).
- [27] R. S. Somerville, K. Lee, H. C. Ferguson, J. P. Gardner, L. A. Moustakas, and M. Giavalisco, Cosmic variance in the great observatories origins deep survey, *Astrophys. J.* **600**, L171 (2004).
- [28] M. Trenti and M. Stiavelli, Cosmic variance and its effect on the luminosity function determination in deep high z surveys, *Astrophys. J.* **676**, 767 (2008).
- [29] B. P. Moster, R. S. Somerville, J. A. Newman, and H.-W. Rix, A cosmic variance cookbook, *Astrophys. J.* **731**, 113 (2011).
- [30] S. Codis, F. Bernardeau, and C. Pichon, The large-scale correlations of multicell densities and profiles: Implications for cosmic variance estimates, *Mon. Not. R. Astron. Soc.* **460**, 1598 (2016).
- [31] E. Krause and T. Eifler, cosmolike—cosmological likelihood analyses for photometric galaxy surveys, *Mon. Not. R. Astron. Soc.* **470**, 2100 (2017).
- [32] D. Gruen, S. Seitz, M. Becker, O. Friedrich, and A. Mana, Cosmic variance of the galaxy cluster weak lensing signal, *Mon. Not. R. Astron. Soc.* **449**, 4264 (2015).
- [33] M. J. White, L. M. Krauss, and J. Silk, Inflation and the statistics of cosmic microwave background anisotropies: From 1-degree to COBE, *Astrophys. J.* **418**, 535 (1993).
- [34] J. Yoo, E. Mitsou, Y. Dirian, and R. Durrer, Background photon temperature \bar{T} : A new cosmological parameter?, *Phys. Rev. D* **100**, 063510 (2019).
- [35] J. C. Pober *et al.*, What next-generation 21 cm power spectrum measurements can teach us about the epoch of reionization, *Astrophys. J.* **782**, 66 (2014).
- [36] A. K. Shaw, S. Bharadwaj, and R. Mondal, The impact of non-Gaussianity on the error covariance for observations of the Epoch of Reionization 21-cm power spectrum, *Mon. Not. R. Astron. Soc.* **487**, 4951 (2019).
- [37] J. B. Muñoz, Robust velocity-induced acoustic oscillations at cosmic dawn, *Phys. Rev. D* **100**, 063538 (2019).
- [38] J. B. Muñoz, Standard Ruler at Cosmic Dawn, *Phys. Rev. Lett.* **123**, 131301 (2019).
- [39] A. Mesinger and S. Furlanetto, Efficient simulations of early structure formation and reionization, *Astrophys. J.* **669**, 663 (2007).
- [40] A. Mesinger, S. Furlanetto, and R. Cen, 21 cmFAST: A fast, semi-numerical simulation of the high-redshift 21-cm signal, *Mon. Not. R. Astron. Soc.* **411**, 955 (2011).
- [41] B. Greig and A. Mesinger, 21 CMMC: an MCMC analysis tool enabling astrophysical parameter studies of the cosmic 21 cm signal, *Mon. Not. R. Astron. Soc.* **449**, 4246 (2015).
- [42] B. Greig and A. Mesinger, Simultaneously constraining the astrophysics of reionization and the epoch of heating with 21 CMMC, *Mon. Not. R. Astron. Soc.* **472**, 2651 (2017).
- [43] Please see Supplemental Material at <http://link.aps.org/supplemental/10.1103/PhysRevD.103.023512> for derivations, additional explanations, and figures related to the results in the main text.
- [44] A. A. Kaurov, T. Venumadhav, L. Dai, and M. Zaldarriaga, Implication of the shape of the EDGES signal for the 21 cm power spectrum, *Astrophys. J.* **864**, L15 (2018).
- [45] K. Tauscher, D. Rapetti, and J. O. Burns, Formulating and critically examining the assumptions of global 21-cm signal analyses: How to avoid the false troughs that can appear in single spectrum fits, *Astrophys. J.* **897**, 132 (2020).
- [46] N. Y. Gnedin, Cosmic reionization on computers I. Design and calibration of simulations, *Astrophys. J.* **793**, 29 (2014).

- [47] P. Ocvirk *et al.*, Cosmic dawn (CoDa): The First radiation-hydrodynamics simulation of reionization and galaxy formation in the local universe, *Mon. Not. R. Astron. Soc.* **463**, 1462 (2016).
- [48] G. B. Poole, P. W. Angel, S. J. Mutch, C. Power, A. R. Duffy, P. M. Geil, A. Mesinger, and S. B. Wyithe, Dark-ages Reionization and Galaxy formation simulation—I. The dynamical lives of high-redshift galaxies, *Mon. Not. R. Astron. Soc.* **459**, 3025 (2016).
- [49] A. Mesinger, B. Greig, and E. Sobacchi, The evolution Of 21 cm structure (EOS): Public, large-scale simulations of Cosmic Dawn and reionization, *Mon. Not. R. Astron. Soc.* **459**, 2342 (2016).